Short Reference Image Quality Estimation Using Modified Angular Edge Coherence

Dmitry V. Sorokin, Andrey S. Krylov

Faculty of Computational Mathematics and Cybernetics

Moscow Lomonosov State University, Moscow, Russia

{dsorokin, kryl}@cs.msu.ru

Abstract

A new short reference image quality metric is introduced in this paper. It is based on the idea that a high quality image has a high value of angular edge coherence in the basic edges points and a low level of angular edge coherence in the basic edges neighborhood. The angular edge coherence is measured using the coefficients of image expansion into the Gauss-Laguerre Circular Harmonic Functions. The practical usability is illustrated with several test images.

Keywords: *Gauss-Laguerre circular harmonic functions, image quality metric, angular edge coherence, basic edges.*

1. INTRODUCTION

The problem of results quality estimation in image enhancement or restoration algorithms does not have an universal solution. The automatic image quality metrics often do not correlate well enough with the perceptual image quality.

There are many approaches which are performed by direct pixel-by-pixel calculation of conventional signal metrics (such as MSE, PSNR, RMSE etc.) of the obtained and the original images. These techniques are referred in the literature as full reference image quality assessment metrics. There are also more sophisticated metrics taking into account perceptual features of human visual system [1].

But for the majority of image processing tasks we cannot use the full reference metrics due to the absence of the reference image. For this reason no-reference (or "blind") methods and short reference methods are designed. No-reference approaches assess the quality of image without any information about original image. Short reference approaches operate with partial information about original image. Some of these methods are introduced in [2-4]. The methods based on the edge coherence approach are introduced in [5,6]. They are based on the local expansion of the observed image into the system of so-called Gauss-Laguerre orthonormal family.

In this paper a new approach using modified angular edge coherence is proposed. The modification is based on Gauss-Laguerre expansions analysis. The importance for the human image perception of the areas near the main image edges has also been taken into consideration.

2. MULTIMODAL ANGULAR EDGE COHERENCE

Let us consider a family of complex orthonormal and polar separable family of functions:

$$g_n^\alpha(r, \gamma; \sigma) = \psi_n^{|\alpha|}(r^2 / \sigma) e^{i\alpha\gamma}.$$

Their radial profiles are Laguerre functions:

$$\psi_n^\alpha(x) = \frac{1}{\sqrt{n!\Gamma(n+\alpha+1)}} x^{\alpha/2} e^{-x/2} L_n^\alpha(x),$$

where $n = 0,1,\ldots; \alpha = 0, \pm 1, \pm 2 \ldots$ and $L_n^\alpha(x)$ are Laguerre polynomials:

$$L_n^\alpha(x) = (-1)^n x^{-\alpha} e^x \frac{d}{dx^n}(x^{n+\alpha} e^{-x}).$$

The Laguerre function $\psi_n^\alpha(x)$ can be calculated using the following recurrence relations:

$$\psi_{n+1}^\alpha(x) = \frac{(x-\alpha-2n-1)}{\sqrt{(n+1)(n+\alpha+1)}} \psi_n^\alpha(x) -$$

$$- \sqrt{\frac{n(n+\alpha)}{(n+1)(n+\alpha+1)}} \psi_{n-1}^\alpha(x), \quad n = 0,1,\ldots,$$

$$\psi_0^\alpha(x) = \frac{1}{\sqrt{\Gamma(\alpha+1)}} x^{\alpha/2} e^{-x/2}, \quad \psi_{-1}^\alpha(x) \equiv 0$$

These functions g_n^α, called Laguerre Gauss circular harmonic (LG-CH) functions, are referenced by integers n (referred by radial order) and α (referred by angular order). The real and imaginary part of g_0^1, g_0^3 and g_0^5 are illustrated in Figure 1.

Figure 1: The real parts of g_0^1, g_0^3 and g_0^5 (upper row) and the imaginary parts of g_0^1, g_0^3 and g_0^5 (lower row).

The LG-CH functions are self-steerable, i.e. they can be rotated by the angle φ using multiplication by the factor $e^{i\alpha\varphi}$. They also keep their shape invariant under Fourier transformation. They are suitable for multiscale and multicomponent image analysis [7].

Let us consider an observed image $I(x, y)$ defined on the real plane R^2. Due to the orthogonality of g_n^α family the image $I(x, y)$ can be expanded in the analysis point x_0, y_0 for fixed σ in Cartesian system as follows:

$$I(x_0, y_0) = \sum_{\alpha=-\infty}^{\infty} \sum_{n=0}^{\infty} c_{\alpha,n} g_n^\alpha(x, y),$$

where

$$c_{\alpha,n} = \int_{-\infty}^{\infty}\int_{-\infty}^{\infty} I(x_0, y_0)(g_n^\alpha(x, y))^* dxdy,$$

and

$$x = x_0 + r\cos\gamma, \ y = y_0 + r\cos\gamma.$$

These coefficients can be calculated at any image point x_0, y_0 by convolution:

$$c_{\alpha,n}(x_0, y_0) = I(x, y) * (g_n^\alpha(-x,-y))^*.$$

Let us consider the convolution results $c_{1,0}(x, y)$, $c_{3,0}(x, y)$ and $c_{5,0}(x, y)$ for LG-CH functions of index orders 1,0 3,0 and 5,0. As it has been shown in [5, 6] the high level of magnitude of $c_{1,0}(x, y)$ corresponds to the edges of the image, while $c_{3,0}(x, y)$ and $c_{5,0}(x, y)$ corresponds to different types of crosses, corners (these values are smaller in the edge points). At the same time it is shown in [6] that for the ideal edge patterns, i.e. unitary step edges passing through x_0, y_0, the arguments of $c_{1,0}(x, y)$ and $c_{3,0}(x, y)$ satisfy the following relation:

$$\arg(c_{3,0}(x_0, y_0)) = 3\arg(c_{1,0}(x_0, y_0)) + \pi.$$

It can be shown that the arguments of $c_{1,0}(x, y)$ and $c_{5,0}(x, y)$ satisfy the analogous relation:

$$\arg(c_{5,0}(x_0, y_0)) = 5\arg(c_{1,0}(x_0, y_0)).$$

This relationship is analogues to the relationship of the odd harmonics of the Fourier expansion for a periodic square waveform (see Figure 2). In our approach we take 3 first odd modes (the work [6] took 2 first odd modes).
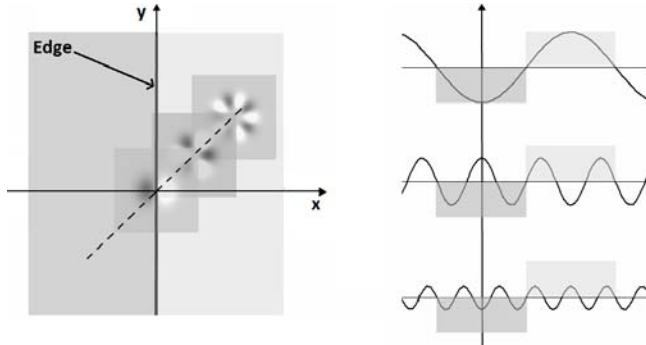
Figure 2: Phase relationship and its analogue with the odd harmonics of the Fourier expansion for a periodic square waveform.

The modified angular edge coherence filter based on these relationships is defined as:

$$MAEC(x_0, y_0) = |c_{1,0}(x_0, y_0)| \cdot$$
$$|\cos(8\arg(c_{1,0}(x_0, y_0)) - \arg(c_{3,0}(x_0, y_0)) - \arg(c_{5,0}(x_0, y_0))$$
$$\cdot (|c_{3,0}(x_0, y_0)||\cos(3\arg(c_{1,0}(x_0, y_0)) - \arg(c_{3,0}(x_0, y_0)))| +$$
$$+ |c_{5,0}(x_0, y_0)||\cos(5\arg(c_{1,0}(x_0, y_0)) - \arg(c_{5,0}(x_0, y_0)))|)$$
.

This approach is more sensitive to the weak edges than the *AEC* [5] (*PEC* [6]). The *AEC* metric (with contrast normalization) is defined in [6] as:

$$AEC(x_0, y_0) = -|c_{1,0}(x_0, y_0)| \cdot |c_{3,0}(x_0, y_0)| \cdot$$
$$\cdot \cos(3\arg(c_{1,0}(x_0, y_0)) - \arg(c_{3,0}(x_0, y_0)))$$
.

It is also important to mention that the value of *MAEC* is positive while the values of *AEC* (*PEC*) can be negative as well. This is crucial for the calculation of *MAEC* for an image region *R*:

$$MAEC_R(I) = \frac{\sum_{(x,y)\in R} MAEC(x, y)}{\|R\|},$$

where $\|R\|$ is the number of points in *R* and the value *MAEC(x,y)* is normalized to lie within [0,1] interval.

3. IMAGE QUALITY METRIC

Standard metrics based on whole image square error calculation like MSE, PSNR do not correlate well with the perceptual image quality. As an example, ringing effect in textured areas is not noticeable while ringing effect near sharp isolated edges is annoying.

In [8] the authors introduced an image quality metrics in edge and edge neighborhood regions for image restoration methods like image interpolation or image deringing. The authors introduced Basic Edge Points (BEP) regions and Basic Edge Neighborhood (BEN) regions in images (see Figure 3). They estimated the quality using RMSE (root of mean square error) of the reference image and the restored image within these areas.

a) Reference image   b) Its BEP (white color) and BEN (grey color) regions

Figure 3: BEP and BEN regions illustration.

In this paper a short reference approach is introduced. This approach is inspired by the fact that *MAEC* value should be reasonably high in BEP regions indicating the good quality of edge restoration. Meanwhile, the values of *MAEC* should be reasonably low in BEN regions indicating the absence of ringing effect. Thus we suggest the following basic edge quality metric:

$$BEQ(I) = \frac{MAEC_{BEP}(I)}{MAEC_{BEN}(I)}$$

Obviously, the specific *BEQ* values correspond to the specific image. For this reason, the relative modification of *BEQ* can be defined as follows:

$$RBEQ(I) = \frac{BEQ(I)}{BEQ(\widetilde{I})}$$

where $I(x, y)$ is observed image and $\widetilde{I}(x, y)$ is the reference image. The *RBEQ* metric is a short reference metric. It analyzes only areas in the region of isolated strong edges. The value of *RBEQ(I)* is less than 1 in case of image quality degradation and greater than 1 in case of image quality improvement.
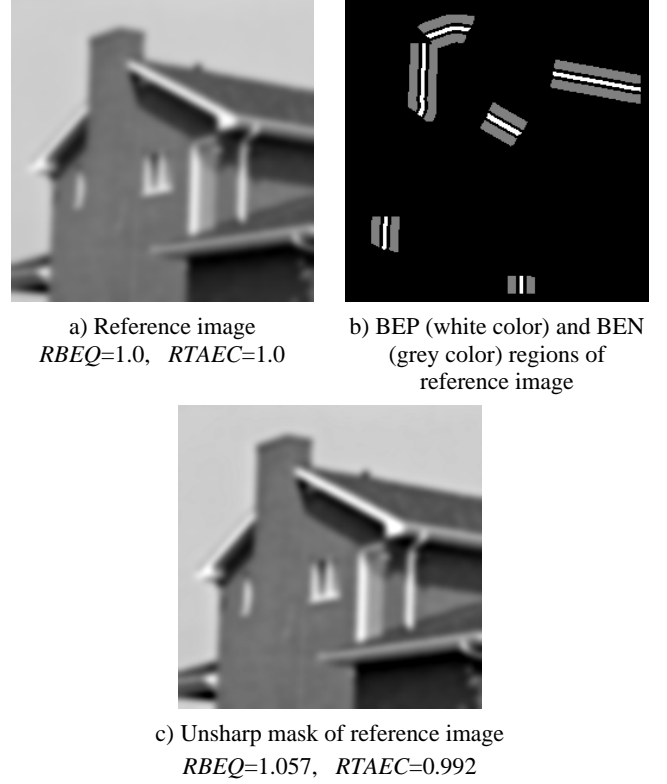
4. EXPERIMENTAL RESULTS

To illustrate the sufficiency of the proposed approach it was tested with different images. The suggested metric has been compared with *RTAEC* metric (the relative short reference metric based on angular edge coherence function for the whole image) [5]. *RTAEC* metric shows good correlation with DMOS results [5]. These results are also close to the results of MSSIM metric.

a) Reference image
RBEQ=1.0,   *RTAEC*=1.0

b) BEP (white color) and BEN (grey color) regions of reference image

c) Reference image with white Gaussian noise
RBEQ=0.530,   *RTAEC*=0.982

d) Gaussian blurred reference image
RBEQ=0.486,   *RTAEC*=0.947

Figure 4: Comparison of *RBEQ* and *RTAEC* metrics.

In Figure 4 ("Lena") and Figure 6 ("Peppers") the reference images, their BEP and BEN map images and corrupted versions of the reference images with different kinds of artifacts are presented. The values of *RBEQ* and *RTAEC* for these images are given. The *RBEQ* metric is more sensitive than *RTAEC* to the image corruption with Gaussian blur, white Gaussian noise and unsharp mask artifacts (see Figures 6d, 6e and 6f). But in the case

of pixelized image the *RBEQ* and *RTAEC* values do not reflect properly the existing artifact (see Figure 6c).

a) Reference image
RBEQ=1.0,   *RTAEC*=1.0

b) BEP (white color) and BEN (grey color) regions of reference image

c) Unsharp mask of reference image
RBEQ=1.057,   *RTAEC*=0.992

Figure 5: Comparison of *RBEQ* and *RTAEC* values for the unsharp masking result

In Figure 5 the result of unsharp mask of blurred "House" image is given. This illustrates the different behavior of *RBEQ* and *RTAEC* metrics. Despite the fact that unsharp mask is enhancing algorithm for blurred images *RTAEC* < 1 indicates the degradation of image quality. On the contrary, *RBEQ* > 1 indicates the improvement in image quality that corresponds to human perception.

It can be seen from the given examples that the *RBEQ* and *RTAEC* metrics both find the blurring of the image but the *RBEQ* is much more sensitive to the presence of noise and it estimates better the unsharp masking results.

In Table 1 the *RBEQ* and *RTAEC* metrics are compared with other types of edge coherence metrics. Where $RBEQ_1$ is defined as:

$$RBEQ_1(I) = \frac{BEQ_1(I)}{BEQ_1(\widetilde{I})}, \quad BEQ_1(I) = \frac{AEC_{BEP}(I)}{AEC_{BEN}(I)},$$
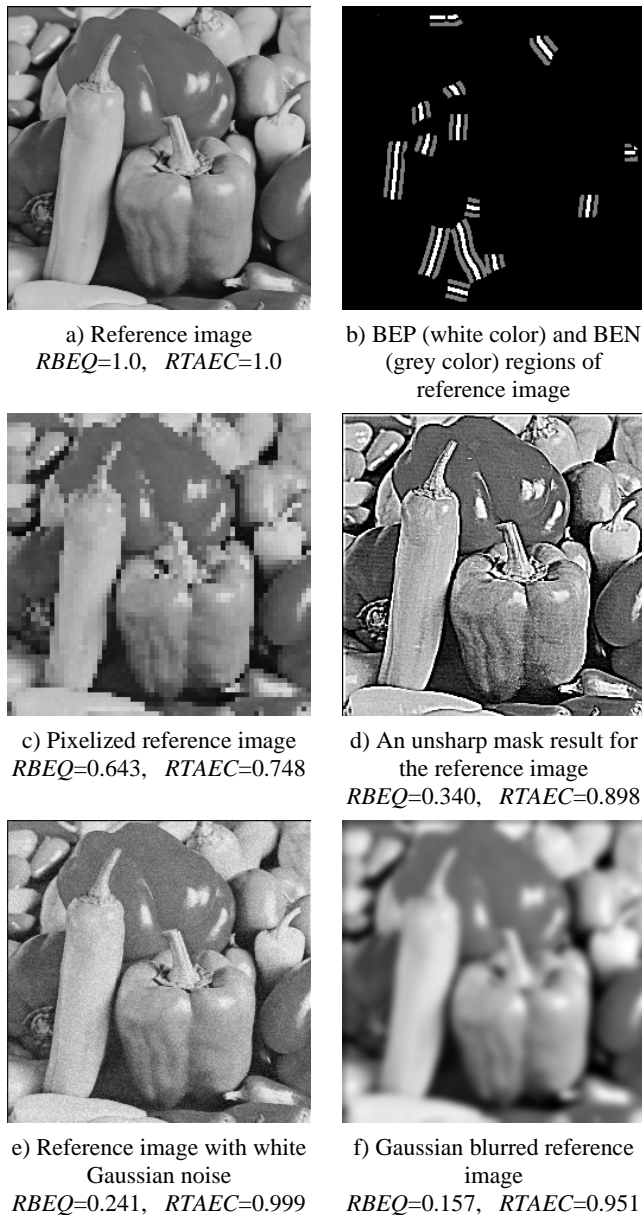
and $RTAEC_1$ is defined as:

$$RTAEC_1(I) = \frac{MAEC(I)}{MAEC(\widetilde{I})}.$$

It is illustrated that $RTAEC_1$ and $RBEQ_1$ metrics are not appropriate. $RTAEC_1 > 1$ in case of image quality degradation and $RTAEC_1 < 1$ in case of image quality improvement. The $RBEQ_1$ metric has the same drawback for images corrupted with white Gaussian noise and it is also less sensitive to the artifacts even in comparison with *RTAEC* metric.

The given results demonstrate the sufficiency of using *MAEC* metric in BEP and BEN regions to construct *RBEQ* image quality metric.

Image	RBEQ	RTAEC	RBEQ₁	RTAEC₁
Figure 4c	0,530	0,982	*1,002*	*1,289*
Figure 4d	0,486	0,947	0,917	*2,707*
Figure 6c	0,643	0,748	0,981	*1,638*
Figure 6d	0,340	0,898	0,950	*2,527*
Figure 6e	0,241	0,999	*1,005*	*1,088*
Figure 6f	0,157	0,951	0,888	*2,776*
Figure 5c	1,057	0,992	1,011	*0,955*

Table 1: Comparison of *RBEQ*, *RTAEC, RBEQ*₁ and *RTAEC*₁ metrics.

a) Reference image
RBEQ=1.0, *RTAEC*=1.0

b) BEP (white color) and BEN (grey color) regions of reference image

c) Pixelized reference image
RBEQ=0.643, *RTAEC*=0.748

d) An unsharp mask result for the reference image
RBEQ=0.340, *RTAEC*=0.898

e) Reference image with white Gaussian noise
RBEQ=0.241, *RTAEC*=0.999

f) Gaussian blurred reference image
RBEQ=0.157, *RTAEC*=0.951

Figure 6: Comparison of *RBEQ* and *RTAEC* metrics.

5. CONCLUSION

A new short reference image quality metric using a modification of the angular edge coherence approach has been developed. The preliminary testing results look promising. The future work will include a detailed statistical analysis of the results for big image bases and a more detailed analysis of specific image artifacts like pixelization.

6. REFERENCES

[1]   M. P. Eckert and A. P. Bradley, "Perceptual quality metrics applied to still image compression"// Signal Processing, v. 70, pp. 177–200, Nov. 1998.

[2]   Z. Whang, E. Simoncelli "Reduced-Reference Image Quality Assessment Using A Wavelet-Domain natural Image Statistic Model" *// Human Vision and Electronic Imaging X, Proc. SPIE 2005, vol. 5666.*

[3]   M. Carnec, P. Le Callet, D. Barba, "Visual Features for Image Quality Assessment with Reduced Reference" *// Proc. of the IEEE ICIP 2005, vol. 1, pp. 421-424.*

[4]   P. Marziliano, F. Dufaux, S. Winkler, T. Ebrahimi, "Perceptual blur and ringing metrics: application to JPEG2000" *// Signal Processing: Image Communication vol. 19, 2004, pp. 163-172.*

[5]   G. L. Capodiferro, E. Di Claudio, G. Jacovitti, "Short Reference Image Quality Rating Based on Angular Edge Coherence" *// Proceedings of 14th European Signal Processing Conference, EUSIPCO 2006, Florence, Italy.*

[6]   V. Baroncini, L. Capodiferro, E. D. Di Claudio, G. Jacovitti, "The polar edge coherence: a quasi blind metric for video quality assessment" *// EUSIPCO 2009, Glasgow, 24-28 Aug. 2009, pp.564-568.*

[7]   Jacovitti, A. Neri, "Multiresolution circular harmonic decomposition" *// IEEE Trans. on Signal Processing, vol. 48, no. 11, 2000, pp. 3242-3247.*

[8]   A. Nasonov, A. Krylov "Adaptive Image Deringing" *// Proc. of GraphiCon'2009, Moscow, Russia, October 2009, pp. 151-154.*

About authors

Dmitry V. Sorokin is postgraduate of the Faculty of Computational Mathematics and Cybernetics, Moscow Lomonosov State University.
Email: dsorokin@cs.msu.ru

Andrey S. Krylov is professor, head of the Laboratory of Mathematical Methods of Image Processing, Faculty of Computational Mathematics and Cybernetics, Moscow Lomonosov State University.
Email: kryl@cs.msu.ru